Supplementary Table 1. Model results under different conditions. Letters in the first column correspond to model results in Figure 2 of the manuscript. Permeability of the seal at the top of the main conduit and of the sides of both conduits were varied for each model run. Fluid input rate was divided evenly across the base of the conduit at different rates for each run. Failure time was computed when overpressure exceeded 5 MPa for each model. Blank cells indicate failure overpressure was never reached. Final overpressure was calculated just below the top seal after three months of model simulation, unless the model ended prematurely in which case the end time in days is indicated in brackets. The simplest models had uniform permeability and porosity, and initial conditions were calculated from Stage 2 run for 200 years. Models were also run with the same properties as the simplest models but with: anisotropic permeability, reduced by one (*k_1*) or two (*k_2*) orders of magnitude laterally within the conduit and seal, and vertically in the host rock; heterogeneous porosity, with conduit 0.3, host rock 0.15, and seals 0.05 (*ϕ_low*) or 0.3 (*ϕ_high*); or with initial conditions calculated from Stage 2 run for 50 years instead of 200 years (*IC 50 yrs*).

	Permeability top seal	**Permeability side seals**	**Fluid input rate**	**Failure time (days)**						**Final Overpressure (MPa)**											
	(log m^2)	(log m^2)	(kg/s)	***Simplest***	***k_1***	***k_2***	***ϕ_low***	***ϕ_high***	***IC 50 yrs***	***Simplest***		***k_1***		***k_2***		***ϕ_low***		***ϕ_high***		***IC 50 yrs***	
a	-12	-14	50							0.0		0.0		0.0		0.0		0.0		0.0	
a	-12	-14	200							0.6		1.6		1.8		0.7		0.7		0.7	
a	-12	-14	500							1.8		4.3		4.7		1.8		1.8		1.4	(45)
	-13	-14	50							1.6		3.3		3.4		1.7		1.6		1.7	
	-13	-14	200		27	24				2.8		13.3		11.6		3.2		2.9		3.3	
	-13	-14	500	58	10	9	46		47	5.6	(65)	18.1	(31)	19.3	(29)	7.1		4.4	(44)	7.1	(83)
	-14	-14	50		71	58				2.3		6.5		7.2		2.3		2.3		2.5	
	-14	-14	200		22	18				3.8		18.6	(71)	36.4		4.0		3.9		4.6	
	-14	-14	500	39	9	8	38	38	33	8.4	(81)	13.5	(12)	74.3	(38)	7.5	(60)	7.2	(61)	9.0	(77)
	-15	-14	50		59	48				2.5		7.3		8.6		2.5		2.5		2.8	
	-15	-14	200		21	16			91	4.2		16.5	(40)	91.1	(54)	4.3		4.3		5.0	
	-15	-14	500	34	9	7	34	34	32	8.0	(61)	13.4	(11)	89.4	(19)	10.0		10.0		10.5	
	-16	-14	50		50	48				2.6		7.6		9.1		2.6		2.6		2.9	
	-16	-14	200		21	16			88	4.3		18.2	(43)	91.4	(49)	4.4		4.4		5.2	
	-16	-14	500	34	9	7	34	34	30	8.1	(61)	13.5	(11)	89.7	(18)	10.3		10.3		10.8	
b	-17	-14	50		52	48				2.6		7.7		9.2		2.6		2.6		2.9	
b	-17	-14	200		21	16			91	4.3		16.6	(38)	91.4	(47)	4.4		4.4		5.2	
b	-17	-14	500	34	9	7	34	34	30	10.0		13.6	(11)	90.1	(18)	10.3		10.3		10.8	
	-12	-15	50							0.0		0.0		0.0		0.0		0.0		0.0	
	-12	-15	200							1.1		1.6		1.7		1.3		1.3		1.1	
	-12	-15	500							3.4		4.3		4.6		3.6		3.8		3.4	

	Permeability top seal (log m²)	Permeability side seals (log m²)	Fluid input rate (kg/s)	Failure time (days)						Final Overpressure (MPa)											
				Simplest	*k_1*	*k_2*	*ϕ_low*	*ϕ_high*	*IC 50 yrs*	*Simplest*		*k_1*		*k_2*		*ϕ_low*		*ϕ_high*		*IC 50 yrs*	
d	-13	-15	50							2.6		3.3		3.4		3.0		2.6		2.5	
d	-13	-15	200	41	27	24	35	48	40	6.6		13.3		12.1		7.1		5.9		6.6	
d	-13	-15	500	16	10	9	15	16	15	13.6		18.1	(31)	19.8	(30)	13.9		15.7		13.6	
	-14	-15	50		71	56				4.2		6.5		7.1		4.4		4.2		4.2	
	-14	-15	200	30	22	17	27	27	29	10.0		18.6	(71)	31.7		10.8		9.8		10.1	
	-14	-15	500	13	9	8	13	13	13	18.7	(76)	13.5	(12)	67.1	(74)	18.9	(87)	18.9	(67)	19.1	(74)
	-15	-15	50		59	49				4.6		7.3		8.3		4.7		4.5		4.6	
	-15	-15	200	26	21	16	25	23	26	10.8		16.5	(40)	86.3	(88)	11.7		10.8		10.9	
	-15	-15	500	12	9	7	13	12	12	19.2	(71)	13.4	(11)	89.2	(22)	19.8	(89)	19.0	(64)	19.6	(71)
	-16	-15	50		50	48				4.7		7.6		8.8		4.8		4.6		4.8	
	-16	-15	200	26	21	16	25	25	26	11.0		18.2	(43)	91.4	(67)	11.9		11.2		11.1	
	-16	-15	500	12	9	8	12	12	12	19.3	(70)	13.5	(11)	89.5	(20)	19.4	(78)	19.3	(65)	19.7	(70)
	-17	-15	50		52	48				4.7		7.7		8.9		4.8		4.7		4.8	
	-17	-15	200	27	21	16	25	25	26	11.1		16.6	(38)	91.4	(63)	12.0		11.2		11.2	
	-17	-15	500	12	9	8	12	12	12	19.3	(70)	13.6	(11)	89.8	(19)	19.8	(85)	19.1	(63)	19.7	(70)
	-12	-16	50							-0.1		0.0		0.0		0.0		0.0		-0.1	
	-12	-16	200							1.6		1.7		1.8		1.7		1.7		1.5	
	-12	-16	500							4.2		4.8		4.7		4.3		4.3		4.1	
	-13	-16	50							3.3		3.5		3.4		4.0		3.2		3.2	
	-13	-16	200	29	27	24	23	27	28	13.2		19.1		11.6		14.8		12.6		12.7	
	-13	-16	500	11	10	9	13	15	11	18.3	(33)	17.6	(27)	19.3	(29)	15.2	(29)	16.4	(31)	18.8	(33)
	-14	-16	50	62	57	58	56	60	60	6.3		7.1		7.2		6.6		6.3		6.5	
	-14	-16	200	23	22	18	19	19	23	18.9		15.8	(34)	36.4		16.2	(61)	17.3	(72)	19.1	(89)
	-14	-16	500	9	9	8	12	12	9	14.4	(14)	12.9	(11)	74.3	(38)	13.4	(19)	14.2	(21)	15.7	(14)
	-15	-16	50	52	50	48	50	52	53	7.1		8.2		8.6		7.1		7.1		7.2	
	-15	-16	200	22	20	16	18	18	21	18.3	(64)	15.7	(30)	91.1	(54)	16.8	(56)	17.1	(60)	17.8	(56)
	-15	-16	500	9	9	7	11	11	9	14.3	(13)	13.3	(11)	89.4	(19)	14.3	(19)	14.2	(19)	13.5	(12)
	-16	-16	50	51	46	48	48	48	48	7.3		8.7		9.1		7.3		7.3		7.5	
	-16	-16	200	21	20	16	18	17	21	17.5	(51)	67.4		91.4	(49)	16.6	(54)	16.8	(56)	17.5	(50)
	-16	-16	500	9	9	7	11	11	9	14.3	(12)	13.5	(10)	89.7	(18)	14.6	(19)	14.6	(19)	13.7	(12)
	-17	-16	50	50	46	48	48	48	48	7.4		8.8		9.2		7.4		7.4		7.6	

	Permeability top seal (log m²)	Permeability side seals (log m²)	Fluid input rate (kg/s)	Failure time (days)						Final Overpressure (MPa)											
				Simplest	***k_1***	***k_2***	***ϕ_low***	***ϕ_high***	***IC 50 yrs***	***Simplest***		***k_1***		***k_2***		***ϕ_low***		***ϕ_high***		***IC 50 yrs***	
	-17	-16	200	22	20	16	18	17	21	17.5	(49)	69.5		91.4	(47)	16.6	(53)	16.6	(54)	17.5	(48)
	-17	-16	500	9	9	7	11	11	9	14.3	(12)	13.5	(10)	90.1	(18)	14.6	(19)	14.6	(19)	13.7	(12)
c	-12	-17	50							-0.1		0.0		0.0		0.0		0.0		-0.1	
c	-12	-17	200							1.6		1.7		1.8		1.9		1.9		1.6	
c	-12	-17	500				24	24		4.6		4.9		4.7		5.0		5.0		4.6	
	-13	-17	50							3.5		3.5		3.4		4.3		3.4		3.5	
	-13	-17	200	28	26	24	22	26	27	17.8		17.1	(78)	11.5		16.2	(81)	16.2	(89)	17.7	
	-13	-17	500	10	10	9	14	14	10	19.2	(30)	18.3	(27)	19.3	(29)	14.5	(23)	13.6	(24)	18.4	(29)
	-14	-17	50	59	55	58	50	54	56	6.8		7.2		7.2		7.5		7.1		7.0	
	-14	-17	200	22	21	17	19	19	22	15.6	(39)	16.9	(35)	37.3		15.9	(50)	15.8	(52)	16.2	(39)
	-14	-17	500	9	9	8	12	12	9	13.6	(12)	12.9	(11)	76.5	(36)	13.8	(18)	13.0	(18)	12.9	(12)
	-15	-17	50	50	52	49	48	46	48	7.7		8.4		8.6		8.2		8.1		8.0	
	-15	-17	200	21	20	16	18	17	21	15.7	(34)	81.9	(89)	91.1	(52)	16.2	(46)	16.5	(47)	15.8	(33)
	-15	-17	500	9	9	7	11	11	9	14.2	(12)	12.8	(10)	89.4	(19)	13.7	(17)	14.3	(18)	69.9	(71)
	-16	-17	50	47	52	48	45	45	49	8.1		8.9		9.2		8.5		8.4		8.4	
	-16	-17	200	21	20	16	16	16	20	15.8	(33)	91.4	(68)	91.4	(47)	16.8	(46)	16.4	(46)	15.7	(32)
	-16	-17	500	9	9	7	11	11	9	70.2	(65)	13.4	(10)	89.8	(18)	13.8	(17)	14.8	(18)	14.6	(11)
e	-17	-17	50	47	52	48	43	47	48	8.1		9.0		9.3		8.5		8.5		8.4	
e	-17	-17	200	21	20	16	16	16	20	15.8	(32)	91.4	(62)	91.5	(46)	16.4	(45)	16.4	(45)	15.8	(32)
e	-17	-17	500	9	9	7	11	11	9	70.1	(64)	13.5	(10)	90.1	(18)	13.9	(17)	14.8	(18)	14.7	(11)

Supplementary Figure 1. Plot of model results with different permeabilities and fluid inputs into the bottom of the conduit. Results are shown for a grid block within the vent directly below the seal (red star in Figure 1). Orange lines with triangles show overpressure, grey dashed lines represent failure overpressure corresponding to a tensile strength threshold of ~5 MPa. Each page corresponds to a different side seal permeability, each row a different top seal permeability, and each column a different basal fluid input rate. If model results exceeded supercritical Waiwera capabilities (>100 MPa, 800 °C) the model ended prematurely as represented by the grey line ending before three months.

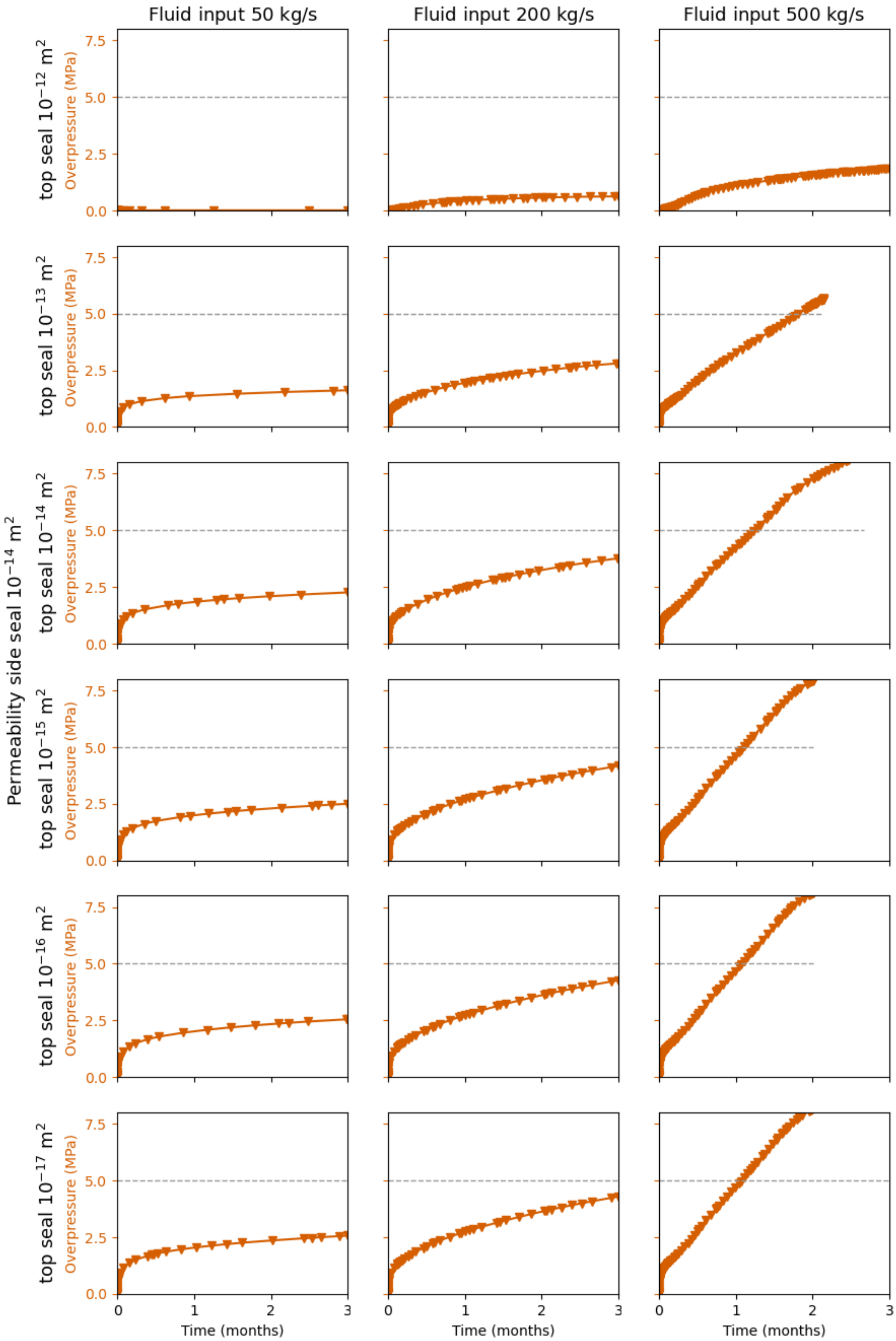
Fluid input 50 kg/s
Fluid input 200 kg/s
Fluid input 500 kg/s
Permeability side seal 10^{-14} m^2
top seal 10^{-12} m^2
top seal 10^{-13} m^2
top seal 10^{-14} m^2
top seal 10^{-15} m^2
top seal 10^{-16} m^2
top seal 10^{-17} m^2
Overpressure (MPa)
Time (months)

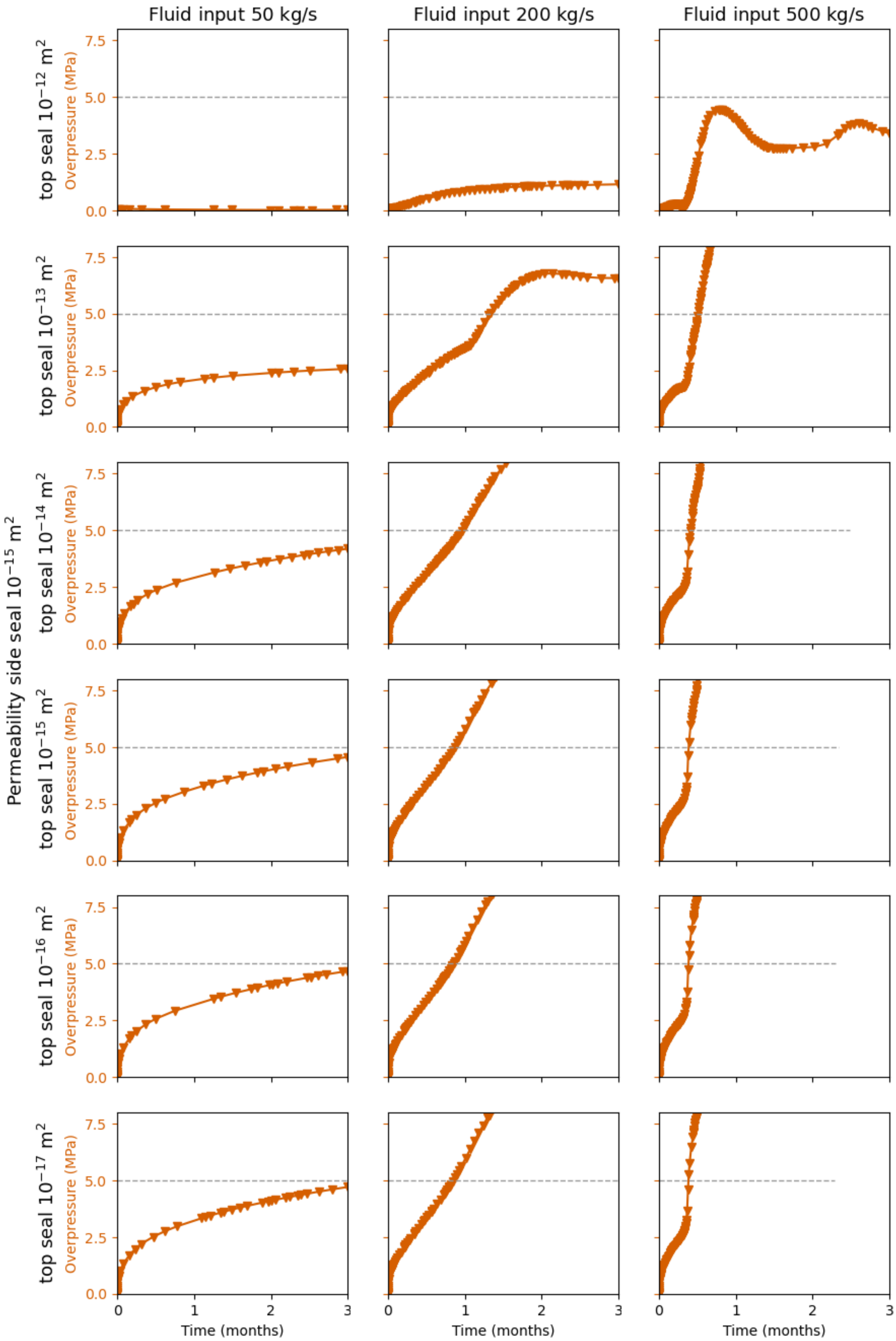
Fluid input 50 kg/s
Fluid input 200 kg/s
Fluid input 500 kg/s
Permeability side seal 10^{-15} m^2
top seal 10^{-12} m^2
top seal 10^{-13} m^2
top seal 10^{-14} m^2
top seal 10^{-15} m^2
top seal 10^{-16} m^2
top seal 10^{-17} m^2
Overpressure (MPa)
Time (months)
0.0
2.5
5.0
7.5
0
1
2
3

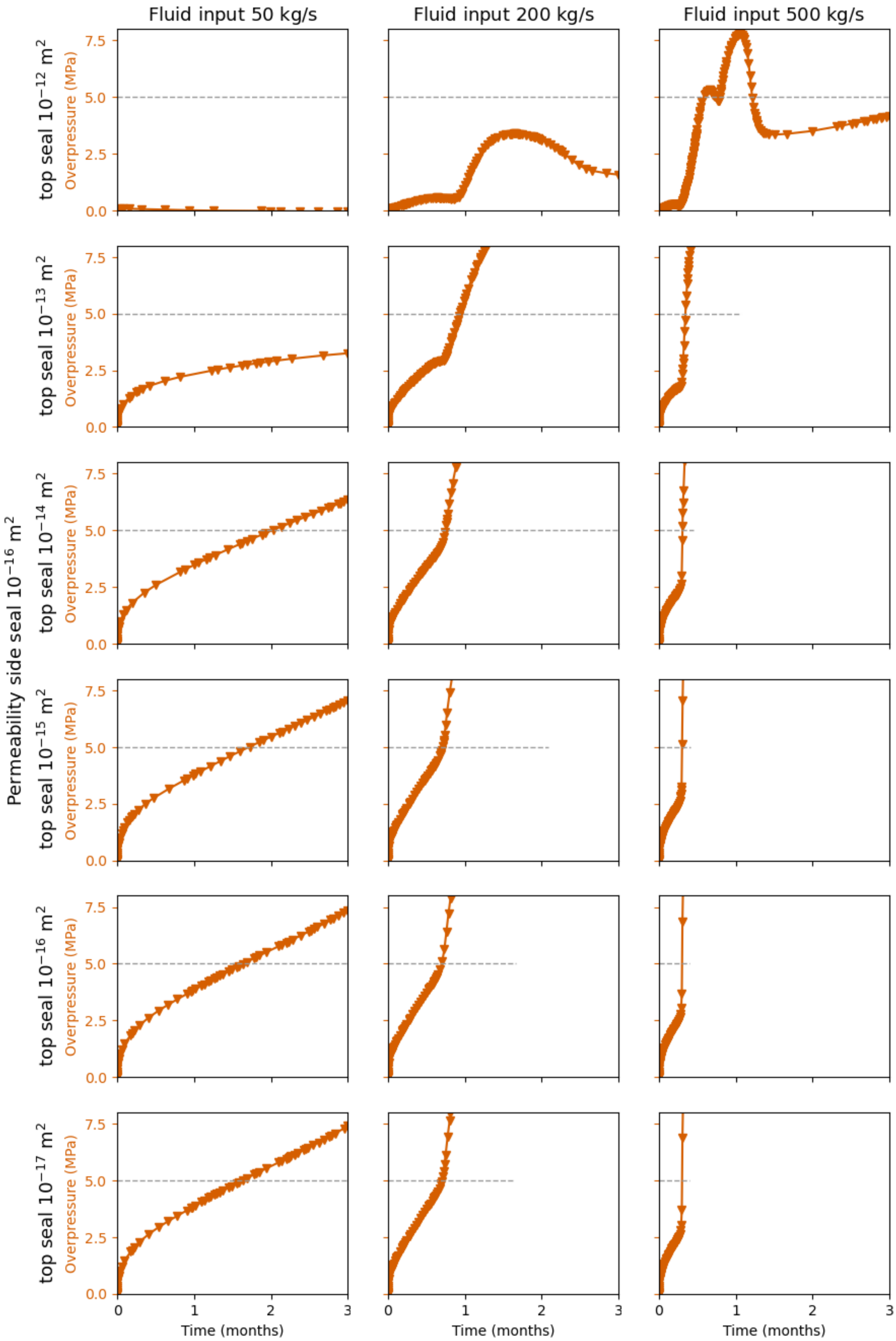

Fluid input 50 kg/s
Fluid input 200 kg/s
Fluid input 500 kg/s
Permeability side seal 10⁻¹⁶ m²
top seal 10⁻¹² m²
top seal 10⁻¹³ m²
top seal 10⁻¹⁴ m²
top seal 10⁻¹⁵ m²
top seal 10⁻¹⁶ m²
top seal 10⁻¹⁷ m²
Overpressure (MPa)
0.0
2.5
5.0
7.5
Time (months)
0
1
2
3

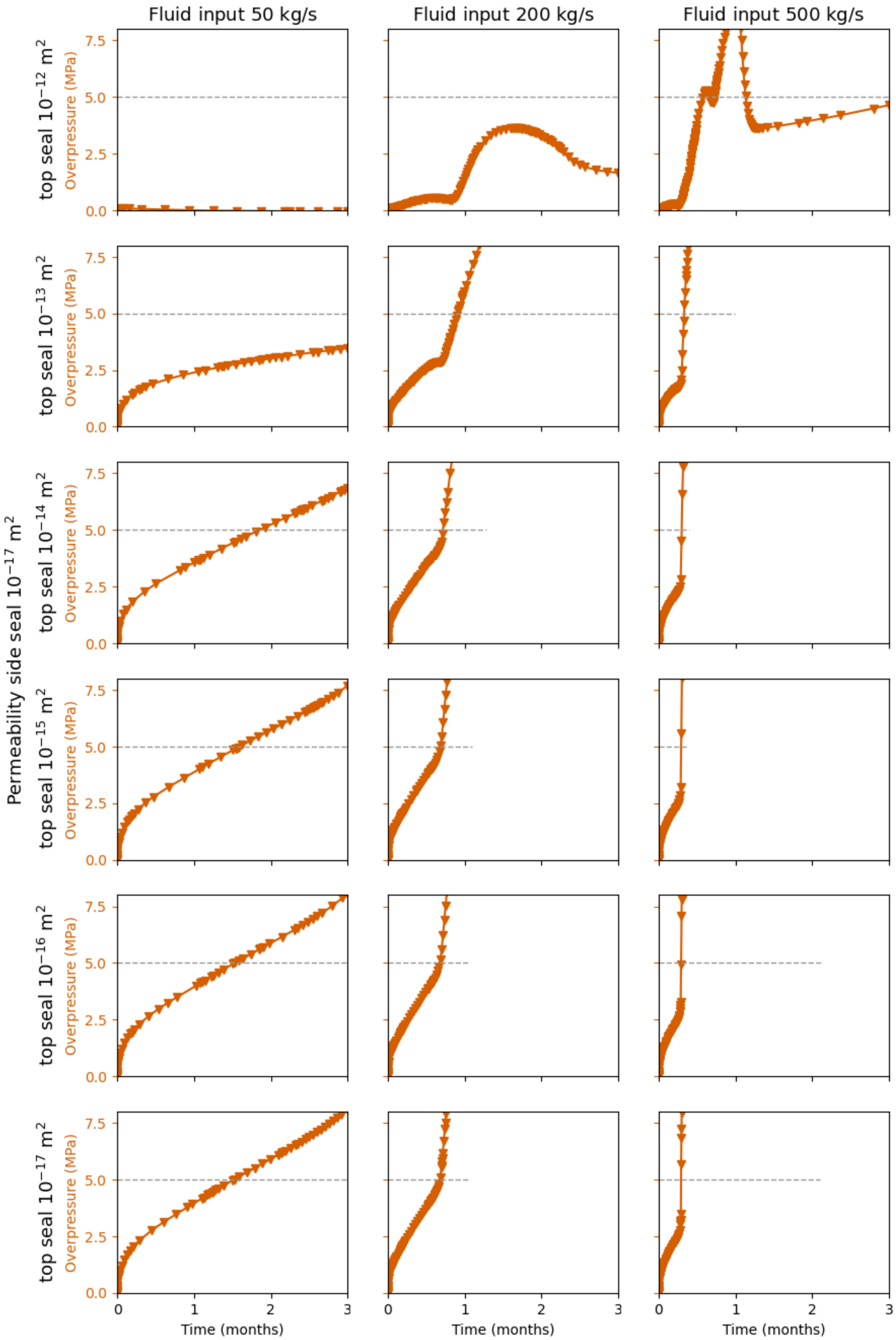

Fluid input 50 kg/s
Fluid input 200 kg/s
Fluid input 500 kg/s
Permeability side seal 10^{-17} m^2
top seal 10^{-12} m^2
top seal 10^{-13} m^2
top seal 10^{-14} m^2
top seal 10^{-15} m^2
top seal 10^{-16} m^2
top seal 10^{-17} m^2
Overpressure (MPa)
0.0
2.5
5.0
7.5
0
1
2
3
Time (months)

Supplementary Figure 2. Model results for different scenarios corresponding to different columns of Supplementary Table 1. Results are from the same model as Figure 4, with top seal permeability of 10^{-14} m^2, side seals permeability of 10^{-15} m^2, and fluid input at 200 kg s^{-1}. Modelled pressure (left), temperature (centre), and vapour saturation (right) are shown after one month, when all models have reached 5 MPa overpressure. **a)** The simplest model, with uniform porosity, isotropic permeability, and Stage 2 run for 200 years. **b)** Stage 2 run for 50 years; all else the same as in (a). Anisotropic permeability was where permeability was reduced by one **(c)** or two **(d)** orders of magnitude horizontally in the conduit and seal, and vertically in the host rock. **e)** With heterogeneous porosity of 0.05 (seals), 0.3 (conduit), and 0.15 (host rock). **f)** With heterogeneous porosity of 0.3 (seals and conduit) and 0.15 (host rock).

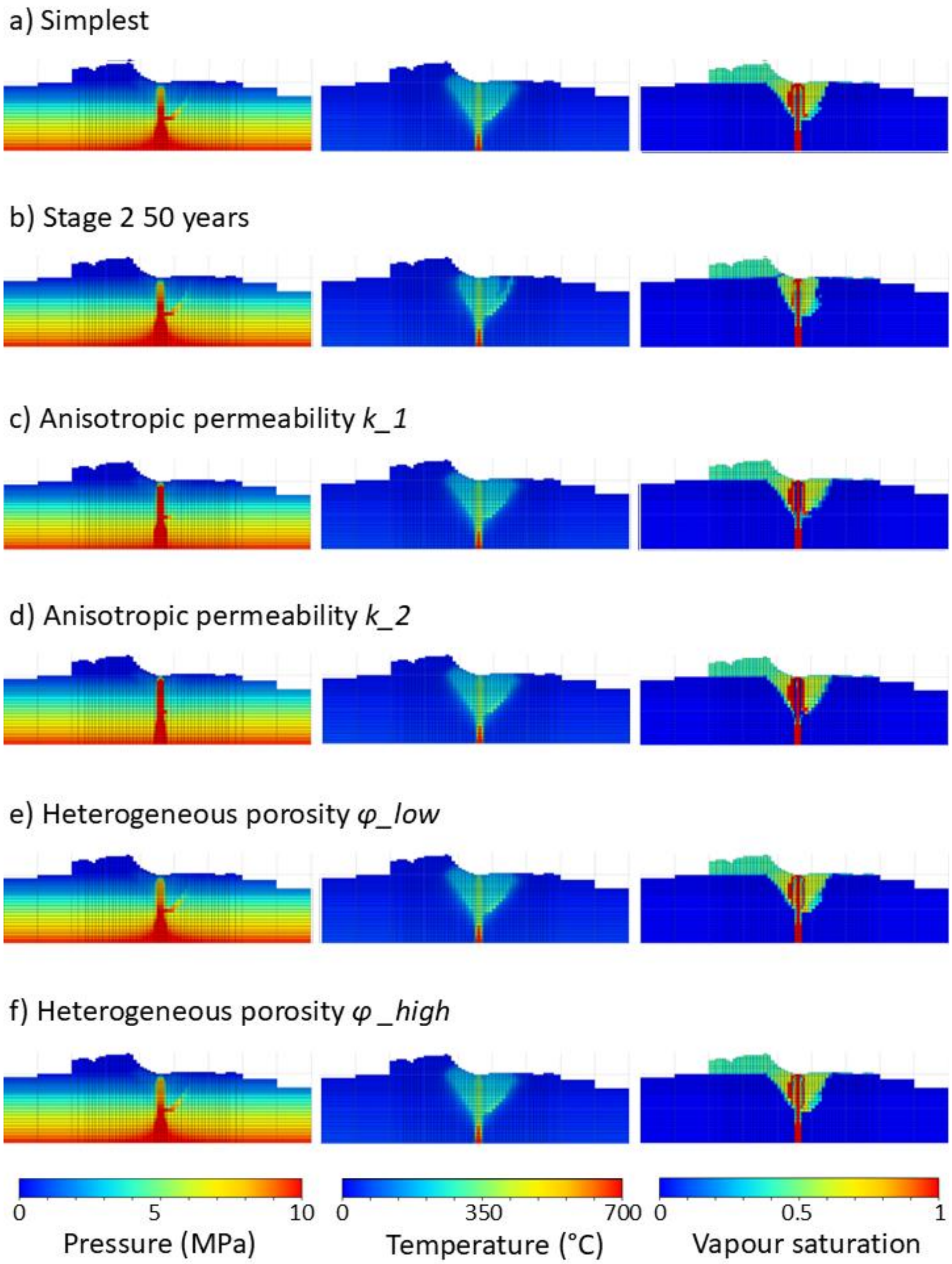

Supplementary Figure 3. Cross-section of Waiwera model grid using TIM visualisation tool. Grid spacing was the same in the perpendicular horizontal direction. Heat was injected across the base of the model (yellow) and hot mass was also injected across the base of the conduit (orange). Cold rainfall was injected into all cells across the top of the model (blues) and the top boundary was set at atmospheric temperature. Aerial blocks (light blue) were set at atmospheric pressure, oceanic blocks (dark blue) at hydrostatic pressure. Vertical boundaries were no-flow.

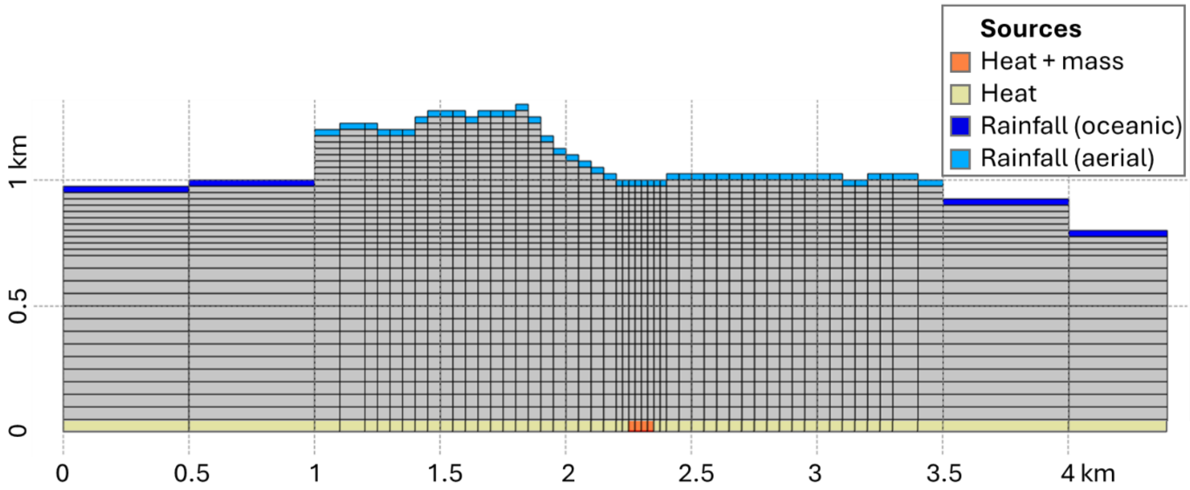

Supplementary Table 2. Simulation parameters used in Waiwera models.

Model parameter	Value or range	Units	Source
Porosity	0.15		Heap et al. 2017; Kennedy et al. 2020
Wet heat conductivity	1.5	W m^{-1} $°C^{-1}$	Simpson 1987
Specific heat capacity	900	J kg^{-1} $°C^{-1}$	Pearson et al. 2014
Permeability host rock	1×10^{-14}	m^2	Heap et al. 2017; Kennedy et al. 2020
Permeability conduit	1×10^{-12}	m^2	Heap et al. 2017; Kennedy et al. 2020
Permeability top seal	1×10^{-17} to 1×10^{-12}	m^2	Heap et al. 2017; Kennedy et al. 2020
Permeability side seals	1×10^{-17} to 1×10^{-14}	m^2	Heap et al. 2017; Kennedy et al. 2020
Basal heat flux	0.1	W m^{-2}	Simpson 1987
Conduit total mass rate	5 to 500	kg s^{-1}	Werner et al. 2008; Burton et al. 2021
Conduit mass enthalpy	3800	kJ kg^{-1}	Kilgour et al. 2021
Rainfall mass input rate	1.93×10^{-6}	Kg s^{-1} m^{-2}	Pearson et al. 2014
Rainfall enthalpy	60	kJ kg^{-1}	Pearson et al. 2014

Supplementary Figure 4. **Model results for different stages of Waiwera hydrothermal modelling.** Initial pressure (left), temperature (centre), and vapour saturation (right) are shown. Vapour saturation is the proportion of air + steam as a fraction of total fluid: above sea level any vapour is air corresponding to the unsaturated zone; below sea level, vapour is predominantly steam. **1)** Initial modelled temperature and pressure were uniform at atmospheric values. The model was run for 1 Myr with fluid input from depth at 5 kg s^{-1} and 350 °C corresponding to the first, long-term stage of hydrothermal activity. **2)** Results of Stage 1. These were used as initial conditions for a model representing increased activity over the last 200 years, with fluid input from depth at 50 kg s^{-1} and 700 °C. **3)** Results from Stage 2, which were used as initial conditions for models of pre-eruptive activity over three months as described in the main body of the text.

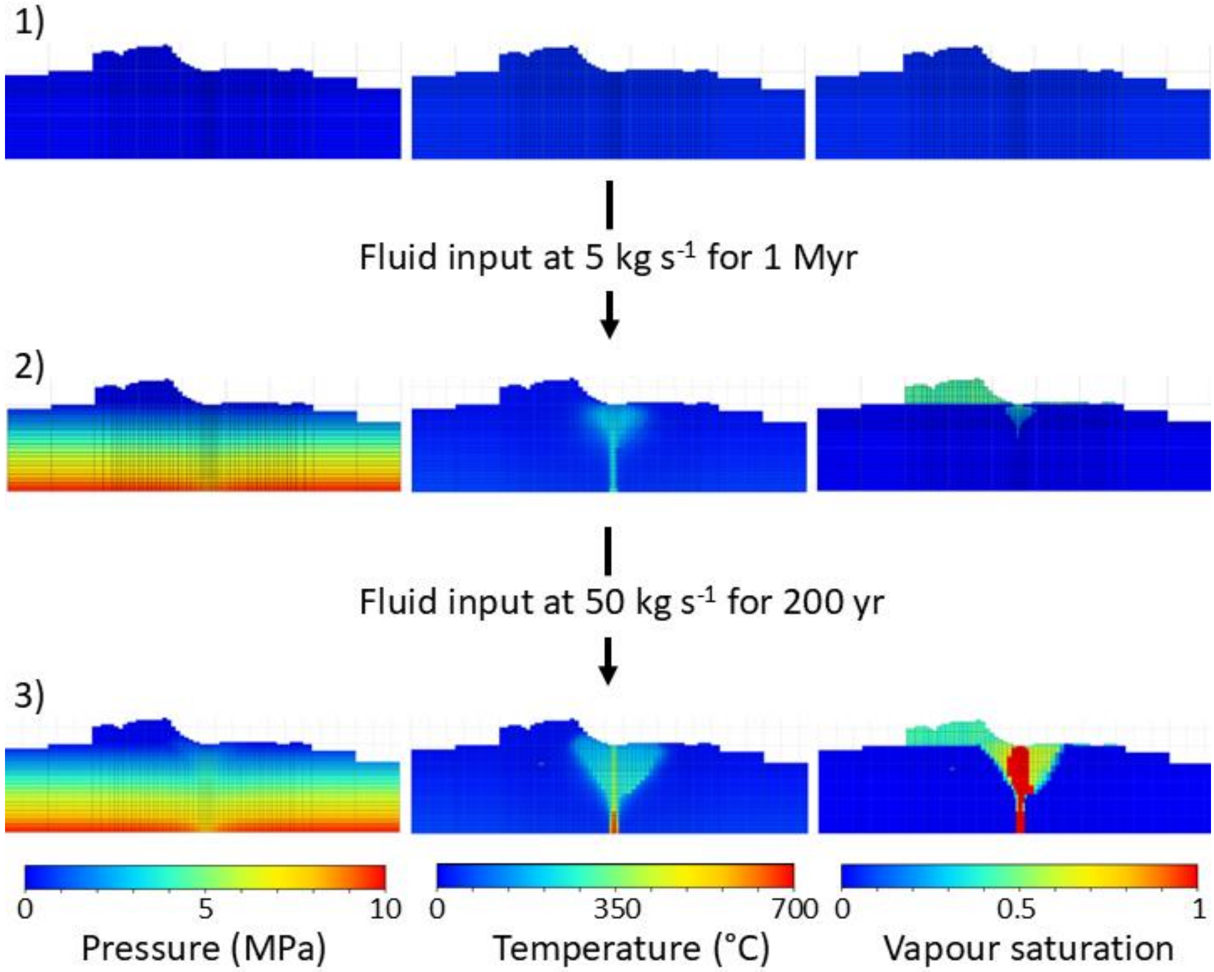

Supplementary References

Burton, M., Hayer, C., Miller, C. & Christenson, B. Insights into the 9 December 2019 eruption of Whakaari/White Island from analysis of TROPOMI SO2 imagery. *Sci Adv* **7**, (2021).

Heap, M. J. *et al.* A multidisciplinary approach to quantify the permeability of the Whakaari/White Island volcanic hydrothermal system (Taupo Volcanic Zone, New Zealand). *Journal of Volcanology and Geothermal Research* **332**, 88–108 (2017).

Kennedy, B. M. *et al.* Pressure controlled permeability in a conduit filled with fractured hydrothermal Breccia reconstructed from ballistics from Whakaari (White island), New Zealand. *Geosciences (Switzerland)* **10**, 138 (2020).

Kilgour, G. N. *et al.* Whakaari/White Island: a review of New Zealand's most active volcano. *New Zealand Journal of Geology and Geophysics* 1–23 (2021) doi:10.1080/00288306.2021.1918186.

Pearson, S. C. P., Alcaraz, S. A. & Barber, J. Numerical simulations to assess thermal potential at Tauranga low-temperature geothermal system, New Zealand. *Hydrogeol J* **22**, 163–174 (2014).

Simpson, B. Heat flow measurements on the bay of plenty coast, New Zealand. *Journal of Volcanology and Geothermal Research* **34**, 25–33 (1987).

Werner, C. *et al.* Variability of passive gas emissions, seismicity, and deformation during crater lake growth at White Island Volcano, New Zealand, 2002–2006. *J Geophys Res Solid Earth* **113**, 1204 (2008).